Nanoscale

Accepted Manuscript

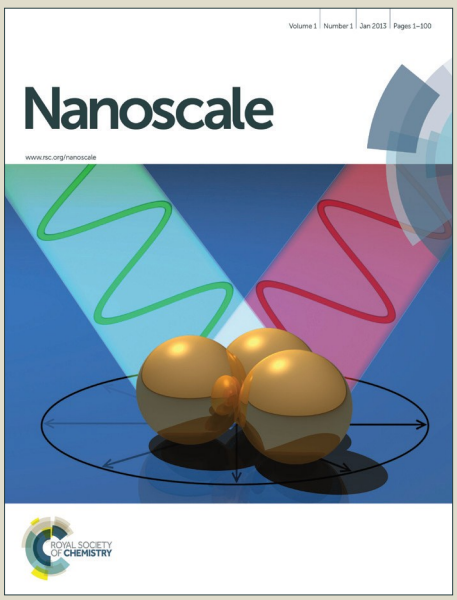

ROYAL SOCIETY OF CHEMISTRY

www.rsc.org/nanoscale

Nanoscale

ARTICLE

Upconversion nanoparticles with a strong acid-resistant capping

Ileana Recalde,[a] Nestor Estebanez,[a] Laura Francés-Soriano,[a] Marta Liras,[b] María González-Béjar,[a]* and Julia Pérez-Prieto.[a]*

Received 00th January 20xx,
Accepted 00th January 20xx

DOI: 10.1039/x0xx00000x

www.rsc.org/

Water-dispersible upconversion nanoparticles (β-$NaYF_4$: Er^{3+},Yb^{3+}, UCNP) coated with a thin shell of a biocompatible copolymer comprising 2-hydroxyethylmethacrylate (HEMA) and 2-acrylamido-2-methyl-1-propanesulphonsulphonic acid (AMPS), which we will term COP, have been prepared by multidentate grafting. This capping is remarkably resistant to strong acidic conditions as low as pH 2. The additional functionality of the smart UCNP@COP nanosystem has been proved by its association to a well-known photosensitizer (namely, methylene blue, MB). The green-to-red emission ratio of the UC@COP@MB nanohybrid exhibits excellent linear dependence in the 7 to 2 pH range as a consequence of the release of the dye as the pH decreases.

Introduction

Upconversion nanoparticles (UCNPs) with an inorganic matrix doped with rare earths (e.g. $NaYF_4$: Er^{3+},Yb^{3+}) have unique photophysical features, such as a large anti-Stokes shift emission after near-infrared (NIR) excitation by using a low-power continuous-wave diode laser. Their excitation at NIR wavelengths considerably reduces background fluorescence, which usually impairs the performance of fluorescence-based assays.[1, 2] In addition, UCNPs do not undergo photobleaching or photoblinking. [1, 2] UCNPs with a hexagonal phase have been extensively used due to their superior upconversion efficiency.[1]

UCNPs are usually coated with organic ligands, typically carboxylates.[3] However, they lose their coating in a medium with a pH below 4, since the carboxylate (e.g., oleate ligand) is protonated and eventually separates from the nanoparticle surface. In fact, this is the strategy used by Capobianco *et al.* to prepare "naked" UCNPs.[3] This capping removal does not only apply to carboxylate ligands but also to ligands anchored via other groups.[4,5-7] It has to be taken into account that the role of the organic capping is not only to determine the dispersibility of a nanoparticle in a specific medium, but also to provide the nanosystem with additional functionality and/or impede the UCNPs from causing any undesirable interference in the environment (such as a cellular environment).[8] This protection is of particular relevance in biological applications.[9]

Organic-capped nanoparticles with the ligand remaining at the nanoparticle surface in a broad range of pHs, and particularly at low pHs (such as that of stomach acid which is close to 2), require high acidic anchoring groups. Sulphonic acids are dramatically more acidic (pK_a ca. -3) than oleic acid and therefore we envisaged that polymers with a high percentage of sulphonate groups could be grafted to the UCNP surface, thus providing a polymer-capped UCNP with high stability not only in a wide range of pHs, but interestingly in highly acidic media. Indeed, the sulphonic group is ionized in virtually the entire range of pHs[10] and the sulphonate group has three potential coordination sites, which allow for more flexible coordination modes and, as a consequence, can form highly flexible frameworks[11, 12] and hydrogen bonding networks.[13, 14] Thus, trivalent lanthanide sulphonates have been used to build clusters,[15] organic extended frameworks,[16] and complexes,[17, 18] as well as polymeric materials.[19] Polystyrene sulphonate/polyallylamine hydrochloride polymer capsules can host lanthanide-doped inorganic nanoparticles (LaF_3:Tb^{3+}, $LaVO_4$:Eu^{3+} and GdF_3:Tb^{3+}) in their hollow cavity.[20]

In addition, the presence of some of the sulphonic groups at the periphery of the polymer-capped UCNP would provide the system with additional functionality, e.g. by covalently linking a pH-probe to give rise to a pH-sensor or by ionic binding to a

[a] Instituto de Ciencia Molecular (ICMol), Universitat de València. Catedrático José Beltrán, 2, 46980 Paterna, Spain
[b] Instituto de Química Orgánica General, Consejo Superior de Investigaciones Científicas (IQOG-CSIC). Juan de la Cierva, 3, 28006 Madrid, Spain. Current address: IMDEA Energy Institute, Parque tecnológico de Móstoles, Avda. Ramón de la Sagra, 3, 28935, Móstoles, Madrid.

Electronic Supplementary Information (ESI) available: [Additional spectra and data of HEMA, AMPS, COP, UCNP@oleate, UCNP@COP, and UCNP@COP@MB]. See DOI: 10.1039/x0xx00000x

drug to generate a pH-responsive drug delivery and release nanosystem.[21] The pH is a key target parameter in a broad range of applications, such as life sciences, food and beverage processing, soil examination, and marine and pharmaceutical research, among others.[22]

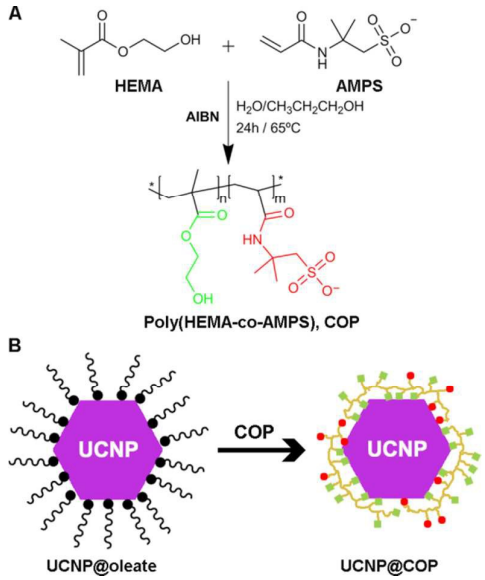

Figure 1. A) Structure of the HEMA and AMPS monomers and the synthesis of the poly(HEMA-co-AMPS) co-polymer (COP). B) Scheme of the synthesis of the functional UCNP@COP nanohybrid.

In particular, water-dispersible UCNPs have recently been proved to be useful for pH measurement and sensing.[23-26] These UCNPs presented a pH-probe (fluorescent or not) embedded in a silica shell or polymer matrix. The probe underwent a spectral shift according to the pH and, as a consequence, the degree of overlap between its absorption and the UCNP emission wavelengths varied, thus resulting in a change in the ratio between the UCNP emission bands.[23, 25] The response to pH reported for these systems was practically linear in the pH-range of 6-11[23, 24] and 3.2-7.2.[25]

We report here the preparation of water-dispersible $NaYF_4$: Er^{3+},Yb^{3+} UCNPs capped with a thin shell of a biocompatible copolymer via sulphonate-grafting (Figure 1). The polymer remained firmly attached under strongly acidic conditions (pH down to 2). As proof of the additional functionality of this polymer-capped UCNP, it was electrostatically bound to a well-known photosensitizer, namely methylene blue (MB). This provided a pH-responsive MB release nanosystem with an excellent linear correlation between the ratiometric photoluminescence of the UCNP and the pH in the 2-7 range.

Results and discussion

Preparation and Characterisation of COP

2-hydroxyethylmethacrylate (HEMA) and 2-acrylamido-2-methyl-1-propanesulphonsulphonic acid (AMPS) have previously been used to obtain highly cross-linked copolymers and hydrogels.[27-30] However, it is possible to minimize the cross-linking and therefore to obtain a water-soluble polymer via free radical polymerization at a moderate temperature by using a high percentage of azobisisobutyronitrile (AIBN) as the initiator[31, 32] (Figure 1). Thus, the synthesis of the poly(HEMA-co-AMPS) co-polymer with an HEMA/AMPS 70:30 molar ratio, here termed COP, was possible due to the difference in reactivity between methacrylate and acrylamide (r_{HEMA}=6.81, r_{AMPS}=0.116)[33] in the free-radical polymerization and by performing a suitable purification protocol, as described by other authors[32] (see Experimental Section).

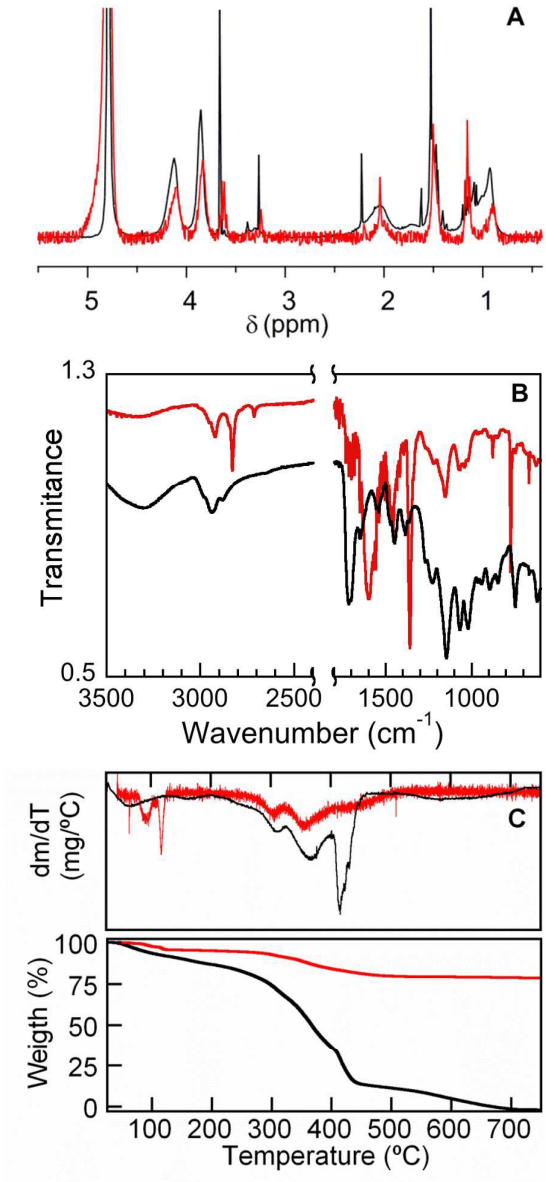

Figure 2. A) ^{1}H-NMR spectra of COP and UCNP@COP in D_2O. B) FTIR-ATR spectra of COP and UCNP@COP. C) TGA analyses and first derivatives of UCNP@COP (Top) and COP (Bottom). Black line: COP; red line: UCNP@COP.

The copolymer was characterised by proton Nuclear Magnetic Resonance (^{1}H-NMR) and Attenuated Total Reflectance Fourier Transform Infrared (FITR-ATR) spectroscopy, and Thermal Gravimetric Analysis (TGA). Figure 2 shows the ^{1}H-NMR and the FTIR-ATR spectra of COP. For comparison, the data of the monomers have been included in the ESI (see Figures S1-S2). The ^{1}H-NMR spectrum of COP matches the one previously reported[31] and illustrates the disappearance of the vinylic signals of HEMA and AMPS monomers (5.6-6.2 ppm, see ESI).

The 70:30 HEMA/AMPS ratio in the poly(HEMA-co-AMPS) co-polymer was confirmed by integrating the CH_2SO_3H and O-CH_2CH_2O methylene protons corresponding to each monomer (see Figure S1 in the ESI for detailed values).

The comparison between the FTIR-ATR spectra of HEMA and AMPS monomers and that of COP also evidenced the generation of the copolymer.[32] Thus, the signals corresponding to carbon double bonds at 1552 cm^{-1}, and the out-of-plane bending peaks that appear in the 1000-650 cm^{-1} range for the AMPS monomer disappear whereas the band between 2800-3000 cm^{-1} is modified due to the CH groups (sp^3 stretch) and a new band at 1452 cm^{-1} can be observed due to the new methylene groups (See Figure 1 and Figure S2 in ESI for comparison with the monomers). Indeed, the two bands of the carbonyl groups (amide and ester) can be observed at 1637 and 1708 cm^{-1}, respectively.

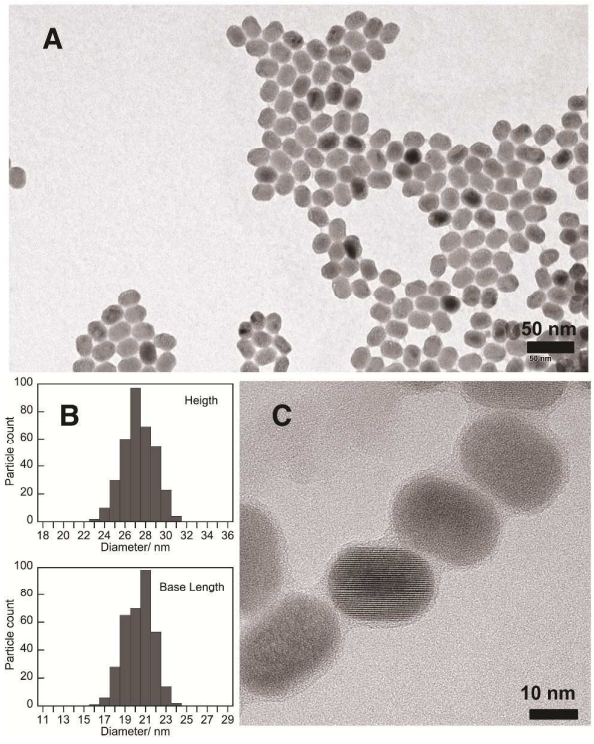

Figure 3. Representative (A) TEM image of UCNP@oleate. (B) Histograms of the of particle size distribution of UCNP@oleate. (C) HRTEM image of UCNP@COP.

Remarkably, the characteristic S=O asymmetric and symmetric stretches of the COP sulphonic groups are observed at 1367 and 1069 cm^{-1}, respectively, while the S-O stretch is found at 671 cm^{-1}. The copolymer had low polydispersity (1.09) and a molecular weight of ~ 19763 g·mol^{-1} (see Table S1 in ESI).

Preparation and Characterisation of the Copolymer-capped UCNP (UCNP@COP)

First, oleate-capped $NaYF_4$:Yb, Er nanoparticles (UCNP@oleate), used as precursors of the copolymer-capped UCNPs (UCNP@COP) were synthesised following a previously reported protocol with some modifications (see ESI).[34, 35] Transmission electron microscopy (TEM) images of UCNP@oleate showed the formation of monodisperse hexagonal nanoprisms with a uniform height of 27.3±1.5 nm, and a base length of 20.5±1.4 nm (Figure 3).

The X-Ray Diffraction (XRD) pattern of the UCNPs revealed the formation of mainly the hexagonal phase structure as bulk β-$NaYF_4$ (Joint Committee on Powder Diffraction Standards, card nº: JCPDS 16-0334), (See Figure S3 in the ESI). The atomic ratios of lanthanides in the nanoparticles were obtained by energy-dispersive X-Ray Experiments (EDX) and were $NaYF_4$(79%):Yb^{3+}(18%),Er^{3+}(3%), see Figure S4.

Then, the UCNP@oleate nanoparticles were treated with COP under basic conditions to perform the ligand exchange (See Experimental part for further details). The resulting system exhibited a high dispersibility in water, thus corroborating the efficient ligand exchange as well as the presence of hydrophilic groups at the nanohybrid periphery.[36]

High-Resolution TEM (HRTEM) images (e.g. Figure 3c) show the UCNP@COP nanohybrid presents a thin polymer shell of a thickness of ca. 1.7±0.3 nm, which is consistent with the copolymer multigrafting to the UCNP surface.

Figure 2 shows the comparison between the ^{1}H-NMR and FITR-ATR spectra, as well as the TGA of UCNP@COP, and those of COP. The ^{1}H-NMR of the UCNP@COP nanohybrid corroborated the efficient exchange of the oleic acid with the copolymer, since no olefinic signals were detected in the spectrum (see Figure S5), and also there was a slight up-field shift of characteristic signals of the copolymer, such as those of $CH_2SO_3^-$ and O-CH_2CH_2O. In addition, the FITR-ATR spectrum revealed significant changes in the band intensity and frequency in the most characteristic bands of COP, such as that of the ester, amide, and sulphonate groups (e.g., see bands at 1723 cm^{-1}, and 1396 cm^{-1}).

These changes are consistent with considerable conformational changes in the polymer after grafting to the UCNP surface as well as with the involvement of some of the above-mentioned groups in the binding. The amount of COP in the nanohybrid was determined by TGA. The weight contribution of the copolymer in the UCNP@COP nanohybrid was *ca.* 20 wt%. The main weight losses (at *ca.* 298°C and 352°C) occurred at similar temperatures to those of COP. However, the typical weight loss at ca. 400°C observed for this kind of copolymers[32] occurred at ca. 430°C for UCNP@COP; this suggests a higher thermal stability of the polymer when

attached to the UCNP surface. The emission spectrum of the UCNP@COP nanohybrid at 980 nm excitation wavelength was registered in water (Figure 4).

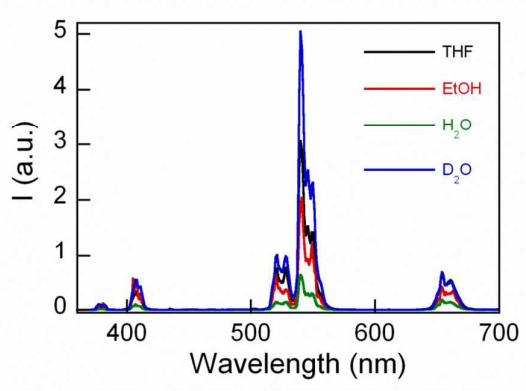

Figure 4. Upconversion emission spectra UCNP@COP: THF (black), EtOH (red), H_2O (green) and D_2O (blue) under 980 nm laser excitation. The spectra were recorded using the same nanoparticle core concentration.

As expected, the upconversion emission spectrum of UCNP@COP showed the typical emissions of the $NaYF_4$: Er^{3+}, Yb^{3+} UCNP[37, 38] (the violet, green, and red upconversion emissions which are characteristic of Er^{3+} and correspond to the $^2H_{9/2}\rightarrow{}^4I_{15/2}$, ($^2H_{11/2}$, $^4S_{3/2}$) $\rightarrow{}^4I_{15/2}$, and $^4F_{9/2}\rightarrow{}^4I_{15/2}$ transitions, respectively). The emission was exactly the same after 2h of irradiation, thus evidencing the photostability of the nanohybrid.

The UCNP@COP nanohybrid was also dispersible in other media, such as THF, ethanol, and D_2O (Figure 4). As previously observed for other water-dispersible UCNPs, the upconversion emission was considerably higher in D_2O than in water, due to differences in energy of the O-H and O-D stretch vibrations that affect the efficiency of the non-radiative deactivation of the lanthanide luminescence.[39]

The capping of the UCNP@COP nanohybrid proved to be stable in a wide range of pHs (from 2 to ca. 10), which is consistent with the involvement of the sulphonate groups in the COP multigrafting. As an example, UCNP@COP nanoparticles were dispersed in water solution at a pH of ca. 2 for 2h and then the nanoparticles were precipitated by centrifugation. The solid was washed with water, centrifuged and dried under vacuum. The FTIR spectrum of the solid corroborated that COP remained anchored to the UCNP surface (see Figure S6). Moreover, measurements of the conductivity and zeta potential of their colloidal solution and of the supernatants from the purification process were consistent with the negligible loss of COP under the acid treatment (see Table S2).

The unusual stability of the UCNP organic capping in strong acid media makes UCNP@COP nanohybrids particularly suitable for many applications where the maintenance of the UCNP capping is crucial for their performance.

It was not expected that all the sulphonate groups would be involved in the COP binding to the UCNP surface, but rather that some would be at the nanohybrid periphery and, consequently, they would progressively protonate when the pH of the medium decreased. Indeed, the zeta potential of UCNP@COP changed from -33 mV at basic conditions (pH ca. 9.5) to -22 mV in the 8 to 3 pH range and became less negative at pHs below 3 (-16 mV at pH ca. 2.5), see Figure 5. These changes are in accordance with those reported for poly(styrene sulphonate)-capped UCNPs[40] and they are consistent with the low pK_a of the sulphonic groups.

The dynamic light scattering (DLS) analysis performed in the same pH range revealed an considerable change in the hydrodynamic diameter (at ca. pH 5), which could be attributed to nanoparticle aggregation at a certain pH/zeta potential.

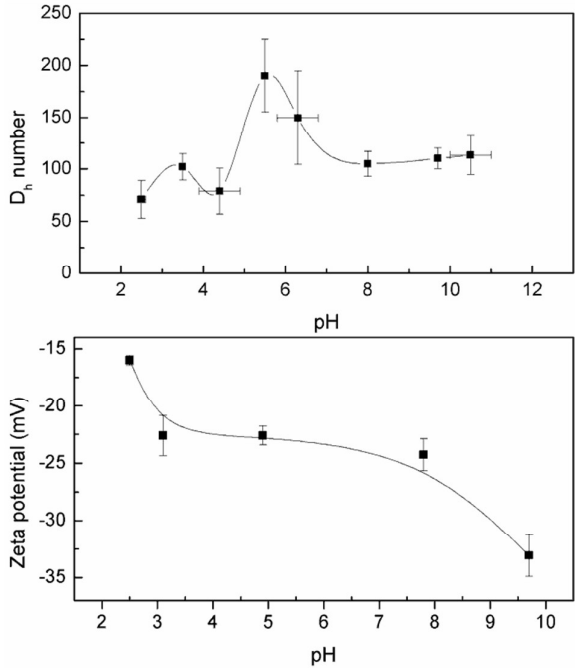

Figure 5. (Top) Dependence of hydrodynamic diameter (D_h) or (Bottom) Zeta Potential vs pH for UCNP@COP dispersed in water (1mg/mL).

In spite of the changes in the hydrodynamic diameter, the emission spectra of UCNP@COP registered at different pHs (from ca. 2 to 13) showed a negligible dependence on the pH (see Figure S7 in ESI).

Building a pH-Responsive MB-Release Nanosystem

UCNP@COP could be electrostatically bound to a cationic molecule by making use of the sulphonate groups at the nanohybrid periphery. Assemblies based on electrostatic attraction have previously been reported.[41] Consequently, the UCNP@COP nanohybrid could be useful to build NIR-responsive nanosystems able to release progressively functional molecules attached to their periphery via competitive binding of H^+ at decreasing pHs, i.e via pH-stimulus.

As a proof of concept we used methylene blue (MB), which is a water-soluble, positively charged cationic dye commonly used as model pollutant to evaluate photocatalytic efficiency [42, 43] or as a photosensitizer for singlet oxygen generation (Figure 6).[44]

The absorption spectrum of MB exhibits a maximum at 660 nm with a shoulder at ca. 550 nm[45] (Figure 7). Its release from the nanohybrid could be observed in a ratiometric fashion taking into account the overlap of the MB absorption spectrum with the red emission of the UCNP. The quenching of such emission would be recovered as MB is released when the H^+ concentration increases.

After several assays to estimate the binding capacity of the UCNP@COP to MB, we eventually prepared the UCNP@COP@MB hybrid by reacting 1.5 nmol of MB per mg of UCNP@COP in water. After stirring the mixture for 2h, the nanoparticles were separated from the solution by centrifugation, washed with water, and finally re-dispersed in water.

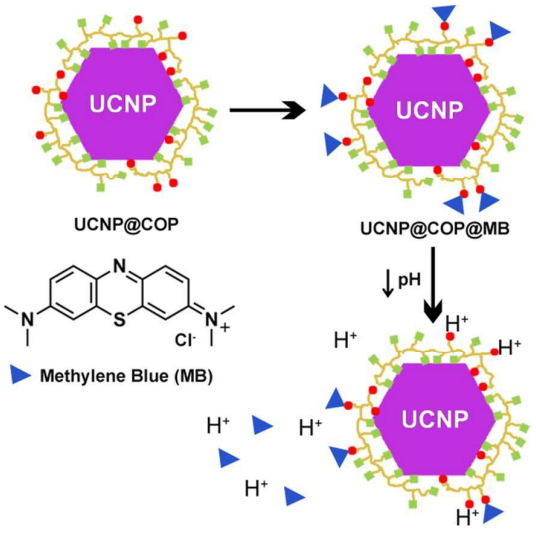

Figure 6. Electrostatic assembly of UCNP@COP and MB to lead to the UCNP@COP@MB nanohybrid, which releases MB as the pH decreases.

Figure 7 compares the absorption of MB and the emission spectra of UCNP@COP and UCNP@COP@MB nanohybrids. Indeed, the absorption spectrum of UCNP@COP@MB showed the typical band of the dye (see Figure S8 in ESI). Taking into account the absorbance of MB in the UCNP@COP@MB and the MB molar absorption coefficient (58,311.9 $M^{-1}cm^{-1}$), the MB amount per 3 mg of UCNP@COP@MB was roughly estimated as 1.8 nmol. In addition, considering that 20% of the weight of UCNP@COP corresponds to COP and 30% of the copolymer is AMPS, the amount of sulphonate in 3 mg of UCNP@COP was estimated as ca. 9 nmol.

Therefore, at least 20% of the sulphonic groups of the copolymer capping are coordinated to MB at a neutral pH and the rest are probably involved in the copolymer grafting to the UCNP surface.

The emission spectrum of UCNP@COP@MB evidenced a decrease in the red-to-green (R/G) emission ratio compared to that in UCNP@COP; this suggests energy transfer from the UCNP to the dye.

The efficiency of the process (η) was calculated as 20% by using a simple formula based on emission intensities (eq. 1)

$$\eta = (I_D - I_{DA})/I_D \quad \text{(eq. 1)}$$

where I_{DA} and I_D are the integrated red emission of UCNP@COP@MB and UCNP@COP nanohybrids.

The spectral overlap integral (J), was calculated as 4.8×10^{12} $nm^4 \cdot M^{-1} \cdot cm^{-1}$ by using the following equation (eq. 2)

$$J = \Sigma\, \sigma_D(\lambda)\sigma_D(\lambda)\lambda^4\delta\lambda \quad \text{(eq. 2)}$$

where σ_D is the normalised donor emission spectrum, λ is the light wavelength, and σ_A is the acceptor molar extinction coefficient.

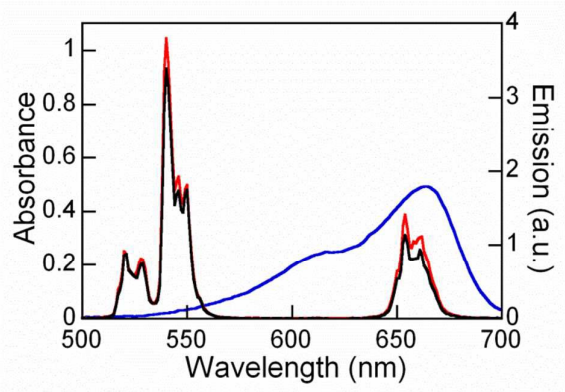

Figure 7. Upconversion emission spectra of UCNP@COP (red line) and UCNP@COP@MB (black line) solutions (1mg/mL) under 980 nm laser excitation in water. MB absorption spectrum has been included for comparison (Blue line).

We next studied the dependence of the R/G emission ratio in UCNP@COP@MB on the pH. No changes were observed in the basic range. Remarkably, a good correlation between this ratio and the pH was observed in the 2-7 pH range (Figure 8). The sample at the lowest pH was centrifuged to determine the degree of MB release at this pH, thus evidencing practically the complete release of MB at this pH.

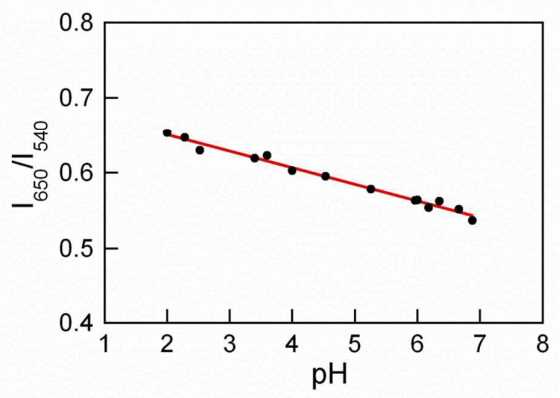

Figure 8. Plot of R/G emission (area under the curve) ratio vs pH for the water-dispersible UCNP@COP@MB nanosystem.

Experimental

Synthesis of COP Copolymer

Briefly, 2-hydroxyethyl methacrylate (HEMA) was purified by column chromatography that contained GC20 grade alumina (Polysciences).The purified monomers were stored in darkness at 4ºC. 2-acrylamide-2-methilpropanesulphonsulphonic (AMPS) was used without previous purification. 2,2'-azobisisobutyronitrile (AIBN) was purchased from Sigma-Aldrich.

Co-polymerization was carried out in a deoxygenated mixture of milli-Q water/n-propanol (50:50 v/v; total volume of 150 mL) containing HEMA (14 mL, 0.1154 mol), AMPS (6g, 0.0289 mol, and AIBN as initiator (600mg, 3.65mmol). So, the HEMA/AMPS molar ratio in the feed was 80:30. The solution was deoxygenated by nitrogen bubbling for 30 min and continuously stirred at 65°C for 24 h. The reaction was stopped by cooling (using an ice-bath), the supernatant was separated, and the organic solvents were removed at reduced pressure. Then, chloroform was added and the mixture was vigorously stirred during 5h. Subsequently, in a separation funnel, the supernatant wet chloroform emulsion was separated and transferred to a centrifuge tube (10000 rpm, 10 min). Three phases were observed, the first denser phase was discarded and the second one was vacuum dried (14g) and characterised as poly(HEMA-co-AMPS) (7:3). This copolymer was used for the UCNP coating.

Synthesis of the Oleate-capped UCNP

$NaYF_4$:Yb (18%), Er (3%) nanocrystals were synthesised following a previously reported protocol with some modifications (See supporting information).

Preparation of the Copolymer-capped UCNP

Firstly, poly(HEMA-co-AMPS) (50 mg) was dispersed in 100 mL of a 70:30 mixture of dichloromethane:tetrahydrofuran (DCM:THF) and constantly stirred for ca. 48h. Once the co-polymer had dispersed, 1g of Na_2CO_3 was slowly added and the mixture was energetically stirred for 2 hours (bubble formation was patent). Then, the co-polymeric solution was decanted in order to eliminate Na_2CO_3. The solid was washed with 10mL of THF and decanted again. The final solution was concentrated by rotary-evaporation. Finally, 10 mg of UCNP were added to a dispersion of 50 mg of COP in 10 mL of THF (5/1 wt. %). The dispersion was vigorously stirred for 24h, and the resulting crude was centrifuged and washed with THF until no polymer was detected by UV in the THF solution, usually 30-60 mL were necessary.

Emission and Dynamic Light Scattering Measurement of the Nanohybrid at Different pHs

The nanohybrid was dispersed in milliQ water (1 mg/mL) and the pH of the colloidal solution was measured. Then, the pH was changed by adding minimal amounts (5µL) of an aqueous solution of sodium hydroxide or HCl solution as required. After each addition, the pH and the emission (as well as, the dynamic light scattering and zeta potential in the case of UCNP@COP) were measured at room temperature. The pH was registered before and after each measurement. Each DLS value was the average of 10-20 independent measurements and an average of 10 rounds.

Conclusions

We report here the synthesis of a NIR-responsive nanohybrid consisting of $NaYF_4$: Er^{3+},Yb^{3+} UCNPs capped with a thin shell of a biocompatible HEMA-AMPS copolymer, which remains firmly anchored to the UCNP due to sulphonate-multigrafting to the UCNP surface. This capping not only remains stable in highly acidic media (as low as a pH of ca. 2), but also enables the UCNP@COP nanohybrid to bind electrostatically to cationic molecules, which can be progressively released when the pH decreases. Therefore, these nanohybrids can be used as functional molecule-release nanosystems. The process can be tracked in a wide range of pHs (from neutral to a pH of ca. 2) by monitoring the nanohybrid emission if the absorption spectrum of the molecule overlaps with some of the emission bands of the UCNP.

Acknowledgements

We thank the Spanish Ministry of Economy and Competitiveness (Projects CTQ2014-60174; Maria de Maeztu: MDM-2015-0538; M.G.B. Ramón y Cajal contract and L.F.S. F.P.U. grant), UE (FP7-PEOPLE, PCIG09-GA-2011, I.R. contract), and UV (VLC-Campus, 02_MCI-26-2015, N.E. contract). We also thank the SCSIE of the University of Valencia for providing access to the NMR, TEM and XRD facilities.

Notes and references

1. A. Gnach and A. Bednarkiewicz, *Nano Today*, 2012, **7**, 532-563.

2. F. Wang, D. Banerjee, Y. Liu and X. C. X. Liu, *Analyst*, 2010, **135**, 1839–1854.

3. N. Bogdan, F. Vetrone, G. A. Ozin and J. A. Capobianco, *Nano Lett.*, 2011, **11**, 835-840.

4. M. Liras, M. González-Béjar, E. Peinado, L. Francés-Soriano, J. Pérez-Prieto, I. Quijada-Garrido and O. García, *Chem. Mater.*, 2014, **26**, 4014-4022.

5. V. Voliani, M. González-Béjar, V. Herranz-Pérez, M. Duran-Moreno, G. Signore, J. M. Garcia-Verdugo and J. Pérez-Prieto, *Chem. Eur. J.*, 2013, **19**, 13538-13546.

6. T. Y. Cao, Y. Yang, Y. Gao, J. Zhou, Z. Q. Li and F. Y. Li, *Biomaterials*, 2011, **32**, 2959-2968.

7. J. P. Yang, D. K. Shen, X. M. Li, W. Li, Y. Fang, Y. Wei, C. Yao, B. Tu, F. Zhang and D. Y. Zhao, *Chem. Eur. J.*, 2012, **18**, 13642-13650.

8. L. Wang and C. Li, *J. Mater. Chem.*, 2011, **21**, 15862-15871.

9. N. Bogdan, E. M. Rodriguez, F. Sanz-Rodriguez, M. a. C. Iglesias de la Cruz, A. Juarranz, D. Jaque, J. G. Sole and J. A. Capobianco, *Nanoscale*, 2012, **4**, 3647-3650.

10. L. Kotin and M. Nagasawa, *J. Am. Chem. Soc.*, 1961, **83**, 1026-1028.
11. B. Xiao, P. J. Byrne, P. S. Wheatley, D. S. Wragg, X. Zhao, A. J. Fletcher, K. M. Thomas, L. Peters, S. O. EvansJohn, J. E. Warren, W. Zhou and R. E. Morris, *Nat. Chem.*, 2009, **1**, 289-294.
12. J. A. Hurd, R. Vaidhyanathan, V. Thangadurai, C. I. Ratcliffe, I. L. Moudrakovski and G. K. H. Shimizu, *Nat. Chem.*, 2009, **1**, 705-710.
13. S. A. Dalrymple and G. K. H. Shimizu, *J. Am. Chem. Soc.*, 2007, **129**, 12114-12116.
14. T. Z. Forbes and S. C. Sevov, *Inorg. Chem.*, 2009, **48**, 6873-6878.
15. F.-Y. Yi, Q.-P. Lin, T.-H. Zhou and J.-G. Mao, *Cryst. Growth Des.*, 2010, **10**, 1788-1797.
16. Q.-Y. Liu, W.-F. Wang, Y.-L. Wang, Z.-M. Shan, M.-S. Wang and J. Tang, *Inorg. Chem.*, 2012, **51**, 2381-2392.
17. P. Thuéry, *Cryst. Growth Des.*, 2012, **12**, 1632-1640.
18. P. Thuéry, *CrystEngComm*, 2012, **14**, 3363-3366.
19. M. J. Tapia and H. D. Burrows, *Langmuir*, 2002, **18**, 1872-1876.
20. H. Sami, A. K. Maparu, A. Kumar and S. Sivakumar, *PLoS One*, 2012, **7**, e36195.
21. J. Liu, Y. Huang, A. Kumar, A. Tan, S. Jin, A. Mozhi and X.-J. Liang, *Biotech. Adv.*, 2013, **32**, 693-710.
22. D. Wencel, T. Abel and C. McDonagh, *Anal. Chem.*, 2014, **86**, 15-29.
23. L.-N. Sun, H. Peng, M. I. J. Stich, D. Achatz and O. S. Wolfbeis, *Chem. Commun.*, 2009, 5000-5002.
24. L. Xie, Y. Qin and H.-Y. Chen, *Anal. Chem.*, 2012, **84**, 1969-1974.
25. R. Arppe, T. Nareoja, S. Nylund, L. Mattsson, S. Koho, J. M. Rosenholm, T. Soukka and M. Schaferling, *Nanoscale*, 2014, **6**, 6837-6843.
26. T. V. Esipova, X. Ye, J. E. Collins, S. Sakadzic, E. T. Mandeville, C. B. Murray and S. A. Vinogradov, *Proc. Natl. Acad. Sci.*, 2012, **109**, 20826-20831.
27. Y. Yuan, R. Liu, C. Wang, J. Luo and X. Liu, *Progress in Organic Coatings*, 2014, **77**, 785-789.
28. M. A. Taleb, D. E. Hegazy and G. A. Mahmoud, *Int. J. Polym. Mater. Po.*, 2014, **63**, 840-845.
29. A. Khabibullin, S. D. Minteer and I. Zharov, *J. Mater. Chem. A*, 2014, **2**, 12761-12769.
30. D. K. Lee, K. J. Lee, Y. W. Kim and J. H. Kim, *Desalination*, 2008, **233**, 104-112.
31. M. R. Aguilar, A. Gallardo, J. San Román and A. Cifuentes, *Macromolecules*, 2002, **35**, 8315-8322.
32. M. R. Aguilar de Armas, Universidad Complutense de Madrid and Instituto de Ciencia y Tecnología de Polímeros, 2002.
33. M. R. Aguilar, A. Gallardo, M. M. Fernández and J. San Román, *Macromolecules*, 2002, **35**, 2036-2041.
34. Z. Zhenquan Li, Y, *Nanotechnology*, 2008, **19**, 345606-345610.
35. V. Voliani, M. Gemmi, L. Frances-Soriano, M. González-Béjar and J. Perez-Prieto, *J. Phys. Chem. C*, 2014, **118**, 11404-11408.
36. Z. Jiang, Y. Shi, Z.-J. Jiang, X. Tian, L. Luo and W. Chen, *J. Mater. Chem. A*, 2014, **2**, 6494-6503.
37. F. Auzel, *Chem. Rev.*, 2004, **104**, 139−173
38. F. Wang and X. Liu, *Chem. Soc. Rev.*, 2009, **38**, 976-989.
39. K. Kogej, S. M. Fonseca, J. Rovisco, M. E. Azenha, M. L. Ramos, J. S. Seixas de Melo and H. D. Burrows, *Langmuir*, 2013, **29**, 14429-14437.
40. L. Wang, R. Yan, Z. Huo, L. Wang, J. Zeng, J. Bao, X. Wang, Q. Peng and Y. Li, *Angew. Chem. Int. Ed.*, 2005, **44**, 6054-6057.
41. J. Peng, W. Xu, C. L. Teoh, S. Han, B. Kim, A. Samanta, J. C. Er, L. Wang, L. Yuan, X. Liu and Y.-T. Chang, *J. Am. Chem. Soc.*, 2015, **137**, 2336-2342.
42. Y. Min, G. He, Q. Xu and Y. Chen, *J. Mater. Chem. A*, 2014, **2**, 1294-1301.
43. S. A. Ansari, M. M. Khan, M. O. Ansari, J. Lee and M. H. Cho, *J. Phys. Chem. C*, 2013, **117**, 27023-27030.
44. J. P. Tardivo, A. Del Glio, C. S. de Oliveira, D. S. Gabrielli, H. C. Junqueira, D. B. Tada, D. Severino, R. F. Turchiello and M. S. Baptista, *Photodiagn. Photodyn. Ther.*, 2005, **2**, 175-191.
45. O. Yazdani, M. Irandoust, J. B. Ghasemi and S. Hooshmand, *Dyes Pigm.*, 2012, **92**, 1031-1041.